Electronic Supplementary Information

Polyoxometalate-based amino-functionalized ionic solid catalysts lead to highly efficient heterogeneous epoxidation of alkenes with H_2O_2

Yan Leng, Jun Wang*, Dunru Zhu, Mingjue Zhang, Pingping Zhao, Zhouyang Long and Jun Huang

State Key Laboratory of Materials-Oriented Chemical Engineering, College of Chemistry and Chemical Engineering, Nanjing University of Technology, Nanjing 210009, China

* Corresponding author, E-mail: junwang@njut.edu.cn

General methods and materials

All chemicals were analytical grade and used as received. FT-IR spectra were recorded on a Nicolet 360 FT-IR instrument (KBr discs) in the 4,000–400 cm^{-1} region. ^{1}H-NMR spectra were measured with a Bruker DPX 300 spectrometer at ambient temperature in D_2O or D^6-DMSO using TMS as internal reference. Electrospray ionization mass spectra (ESI-MS) were recorded with a Finnigan mat APISSQ 710 mass spectrometer. Elemental analyses were performed on a CHN elemental analyzer (FlashEA 1112). Melting points were determined using an X4 digital microscopic melting point apparatus with an upper limit of 250 °C. ESR spectra were recorded on a Bruker EMX-10/12 spectrometer at X-band. The measurements were done at 163 K in a frozen solution provided by a liquid/gas nitrogen temperature regulation system controlled by a thermocouple located at the bottom of the microwave cavity within a Dewar insert. Solid UV-vis spectra were measured with a PE Lambda 950 spectrometer, and $BaSO_4$ was used as an internal standard. XRD patterns were collected on the Bruker D8 Advance powder diffractometer using Ni-filtered Cu Kα radiation source at 40 kV and 20 mA, from 5 to 80 ° with a scan rate of 2 °/min, and before measurements the samples were dried at 100 °C for 2 h. SEM image was performed on a HITACHI S-4800 field-emission scanning electron microscope. BET surface areas were measured at

the temperature of liquid nitrogen using a Micromeritics ASAP2010 analyzer. The samples were degassed at 150 °C to a vacuum of 10^{-3} Torr before analysis. TG analysis was carried out with a STA409 instrument in dry air at a heating rate of 10 °C/min.

Preparation of catalysts

[3-Aminoethyl-1-methylimidazolium]Br ([MimAM]Br): The amino-containing ionic liquid (IL) [MimAM]Br was prepared according to the literature (E. D. Bates, R. D. Mayton, I. Ntai, J. H. Davis, Jr, *J. Am. Chem. Soc.* **2002**, *124*, 926-927). Methylimidazole (8.21 g, 0.10 mol) and 2-bromoethylamine hydrobromide (20.49 g, 0.10 mol) were dissolved in acetonitrile (50 mL) at 80°C for 12 h under nitrogen atmosphere with stirring. On completion, the solvent was removed by distillation, and the residue was recrystallized in ethanol to afford the [MimAM]Br·HBr as a white solid. KOH was added into the aqueous solution of the above solid for neutralization, followed by the evaporation under vacuum. Methanol (20 mL) and $CHCl_3$ (2 mL) were added into the resulting mixture with the appearance of precipitated salts. After filtration, the filtrate was evaporated to give the [MimAM]Br product as yellow oil (Yield: 60%). [PyAM]Br was prepared accordingly.

[3-Piperidylethyl-1-methylimidazolium]Cl ([MimPD]Cl): Methylimidazole (8.21 g, 0.10 mol) and chloroethyl piperidine hydrochloride (18.41 g, 0.10 mol) were dissolved in ethanol (50 mL) at 80°C for 3 days with stirring. The resulting solution was concentrated under vacuum and then washed with CH_2Cl_2 to give the [MimPD]Cl·HCl as a white solid. The subsequent steps were same as those of the above [MimAM]Br. 1-*n*-butyl-3-methylimidazolium bromide ([Bmim]Br) was synthesized according to the previous literature (J. Dupont, C. S. Consorti, P. A. Z. Suarez, R. F. de Souza, *Org. Syn.* **2000**, *79*, 236-240).

The obtained IL [MimAM]Br (1.21 g, 6.0 mmol) was added to an aqueous solution of $H_3PW_{12}O_{40}$ (5.76 g, 2.0 mmol), and then the mixture was stirred at room temperature for 24 h. The formed jade-green precipitate (designated as MimAM(H)-PW) was filtered and washed with water for three times, followed by drying in a vacuum. MimAM(H)-PW was characterized by FT-IR, ^{1}H NMR, ESI-MS, elemental analysis, UV-vis, ESR, TG, SEM, BET surface area and XRD. PyAM(H)-PW, MimPD(H)-PW, and $[Bmim]_3PW$ were synthesized accordingly. $[MimAMH]_{1.5}PW$ was synthesized by reacting [MimAM]Br and $H_3PW_{12}O_{40}$ with the stoichiometric molar ratio of 1.5:1, and $[MimAM]_3PW$ was prepared by reacting [MimAM]Br and sodium phosphotungstate ($Na_3PW_{12}O_{40}$) with the molar ratio of 3:1.

Typical procedure for epoxidation with H_2O_2

Cyclooctene (10 mmol), CH_3CN (10 mL), and MimAM(H)-PW (0.1 g, 0.03 mmol) were added to a 25 mL flask. The reaction started after the addition of aqueous H_2O_2 (30 wt%, 4 mmol) at 70°C within 10 min under vigorous stirring. After the reaction, the reaction mixture was analyzed by gas chromatography (GC). The catalyst was recovered by filtration and washed with ethanol, then dried in vacuum to provide the recovered catalyst, and finally reused in the next run without addition of any fresh catalyst.

Characterization of the synthesized hybrids

MimAM(H)-PW ($[MimAMH]^{2+}_{0.7}[MimAM]^{+}_{1.6}PW_{12}O_{40}^{3-}$): Yield: 96%. m.p.: > 250 °C. BET surface area: 9.89 $m^2 \cdot g^{-1}$. Elemental analysis Calcd for MimAM(H)-PW ($C_{13.8}H_{28.3}N_{6.9}O_{40}PW_{12}$): C, 5.23; H, 0.90; N, 3.05. Found: C, 5.13; H, 0.84; N, 3.19. FT-IR (ν, KBr): 3454s, 3153w, 1626w,

1451w, 1100m, 1080s, 1047m, 979s, 955s, 896s, 806vs, 623w cm^{-1} (**Figure S3B**). ^{1}H NMR (300 MHz, D^{6}-DMSO, TMS); δ 2.86 (m, 2H, $-CH_2$), 3.34 (b, $-NH_2$), 3.88 (s, 3H, $-CH_3$), 4.42 (m, 2H, $-CH_2$), 7.69 (d, 2H, 2(-CH)), 9.07 (s, 1H, -CH). Positive-ion electrospray ionization mass spectrometry (ESI-MS) *m/z*: 126.1 $[MimAM]^{+}$, 83.3 $[MimAMH]^{2+}$·0.5DMSO (**Figure S1A**). Negative-ion electrospray ionization mass spectrum showed a fragmentation pattern identical to that of $PW_{12}O_{40}^{3-}$ **(Figure S1B)**, which is suggested to be an artifact of the electron spray ionization method (Ettedgui, J. Neumann, R. *J. Am. Chem. Soc*. **2009**, *131*, 4-5). The following tentative assignments of the clusters can be made: $H_3PW_4O_{18}/4$ for m/z = 264.3; $H_3W_7O_{25}$ for m/z = 337.9; $H_3PW_6O_{24}/4$ for m/z = 380.3; $HW_5O_{17}/3$ for m/z = 397.4; $PW_{10}O_{35}/5$ for m/z = 485.8.

MimPD(H)-PW ($[MimPDH]^{2+}_{0.8}[MimPD]^{+}_{1.4}PW_{12}O_{40}^{3-}$): Yield: 97%. m.p.: > 250 °C. BET surface area: 9.91 $m^2 \cdot g^{-1}$. Elemental analysis Calcd for MimPD(H)-PW ($C_{24.2}H_{44.8}N_{6.6}O_{40}PW_{12}$): C, 8.79; H, 1.37; N, 2.80. Found: C, 8.39; H, 1.28; N, 2.65. FT-IR (ν, KBr): 3457s, 3149w, 1630w, 1451w, 1100m 1080s, 1047m, 979s, 955s, 896s, 806vs, 623w cm^{-1} (**Figure S8**). ^{1}H NMR (300 MHz, D^{6}-DMSO, TMS); δ 1.57-1.73 (b, 6H, 3($-CH_2$)), 3.11 (b, 4H, 2($-CH_2$)), 3.44 (b, 2H, $-CH_2$), 3.97 (s, 3H, $-CH_3$), 4.57 (b, s, 2H, $-CH_2$), 7.74-7.77 (d, 2H, 2(-CH)), 9.12 (s, 1H, -CH). Positive-ion electrospray ionization mass spectrometry (ESI-MS) *m/z*: 194.1 $(MimPD)^{+}$ (**Figure S6A**). Negative-ion electrospray ionization mass spectrum showed a fragmentation pattern identical to that of $PW_{12}O_{40}^{3-}$ **(Figure S6B)**, which is suggested to be an artifact of the electron spray ionization method (Ettedgui, J. Neumann, R. *J. Am. Chem. Soc*. **2009**, *131*, 4-5). The following tentative assignments of the clusters can be made: $H_3PW_4O_{18}/4$ for m/z = 264.3; $H_3W_4O_{15}/4$ for m/z = 326.1; $H_3PW_6O_{24}/4$ for m/z = 380.3; $HW_5O_{17}/3$ for m/z = 397.4; $HPW_8O_{29}/4$ for m/z = 491.6.

PyAM(H)-PW ($[PyAMH]^{2+}_{0.8}[PyAM]^{+}_{1.4}PW_{12}O_{40}^{3-}$): Yield: 95%. m.p.: > 250 °C. BET surface area: 9.62 $m^2 \cdot g^{-1}$. Elemental analysis Calcd for PyAM(H)-PW ($C_{15.4}H_{25}N_{4.4}O_{40}PW_{12}$): C, 5.87; H, 0.80; N, 1.96. Found: C, 5.59; H, 0.75; N, 1.92. FT-IR (ν, KBr): 3451s, 3134w, 1635w, 1489w, 1100m, 1080s, 1047m, 979s, 955s, 896s, 806vs, 680w cm^{-1} (**Figure S9**). ^{1}H NMR (300 MHz, D^6-DMSO, TMS); δ3.36 (b, $-NH_2$), 3.47 (s, 2H, $-CH_2$), 4.81 (s, 2H, $-CH_2$), 8.21 (s, 2H, 2(-CH)), 8.65 (s, 1H, -CH), 9.00 (s, 1H, 2(-CH)). Positive-ion electrospray ionization mass spectrometry (ESI-MS) *m/z*: 123.3 $(PyAM)^+$, 83.3 $[MimAMH]^{2+}\cdot 0.5DMSO$ (**Figure S7A**). Negative-ion electrospray ionization mass spectrometry (ESI-MS) *m/z*: 957.9 $PW_{12}O_{40}^{3-}$ (**Figure S7B**).

Table S1. Catalytic performance of various catalysts for epoxidation of alkenes with H_2O_2 [a]

Entry	Substrate	Catalyst	Solubility in reaction	C [b] /%	S [c] /%
1	Cyclohexene	$H_3PW_{12}O_{40}$	Soluble	28.7	32.4
2	Cyclohexene	$[Bmim]_3PW$	Soluble	33.9	57.4
3	Cyclohexene	MimAM(H)-PW	Insoluble	90.2	85.5
4	Cyclohexene	PyAM(H)-PW	Insoluble	84.5	62.3
5	Cyclohexene	MimPD(H)-PW	Insoluble	79.0	67.8
6	1-octene	$H_3PW_{12}O_{40}$	Soluble	1.7	48.6
7	1-octene	$[Bmim]_3PW$	Soluble	5.8	83.5
8	1-octene	MimAM(H)-PW	Insoluble	70.5	96.4
9	1-octene	PyAM(H)-PW	Insoluble	59.4	95.6
10	1-octene	MimPD(H)-PW	Insoluble	31.4	100
11	1-hexene	$H_3PW_{12}O_{40}$	Soluble	0	—
12	1-hexene	$[Bmim]_3PW$	Soluble	0	—
13	1-hexene	MimAM(H)-PW	Insoluble	66.1	92.0
14	1-hexene	PyAM(H)-PW	Insoluble	62.3	92.3
15	1-hexene	MimPD(H)-PW	Insoluble	25.4	100

[a] Reaction conditions: catalyst (0.1 g), substrate (10 mmol), 30% H_2O_2 (4 mmol), acetonitrile (10 mL), 70 °C, 6 h for cyclohexene, 8 h for 1-octene and 1-hexene. [b] Conversion of the substrate based on H_2O_2. [c] Selectivity for the epoxide product; byproducts for entries 1-5: 2-cyclohexen-1-ol and 2-cyclohexen-1-one; 6-9: 2-octanone and octylaldehyde; 13 and 14: hexylaldehyde.

Supplementary figures

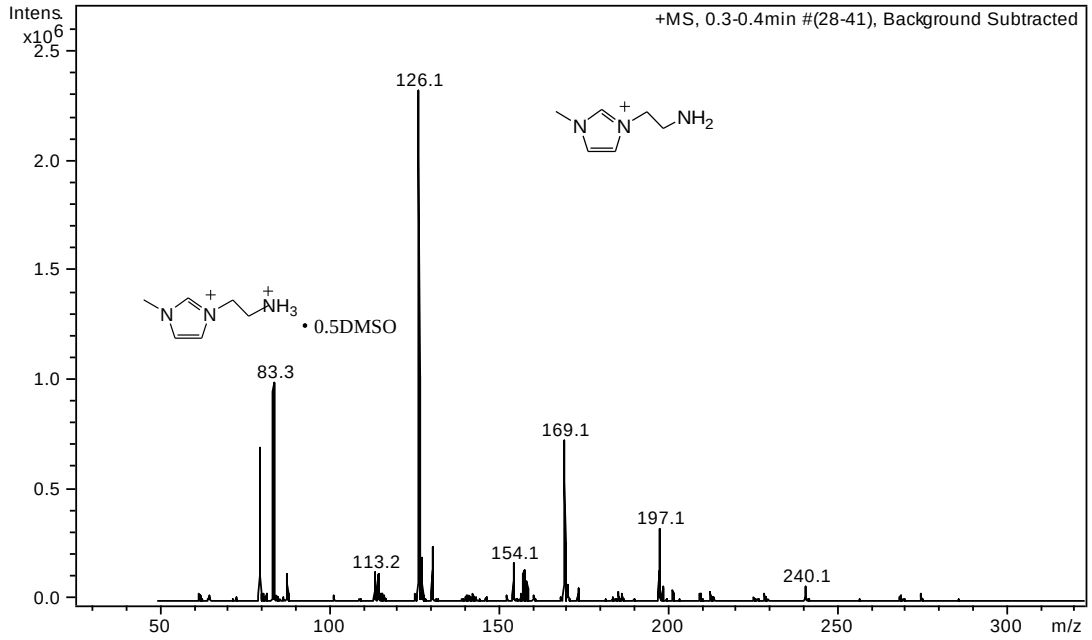

Figure S1A Positive-ion ESI-MS of MimAM(H)-PW

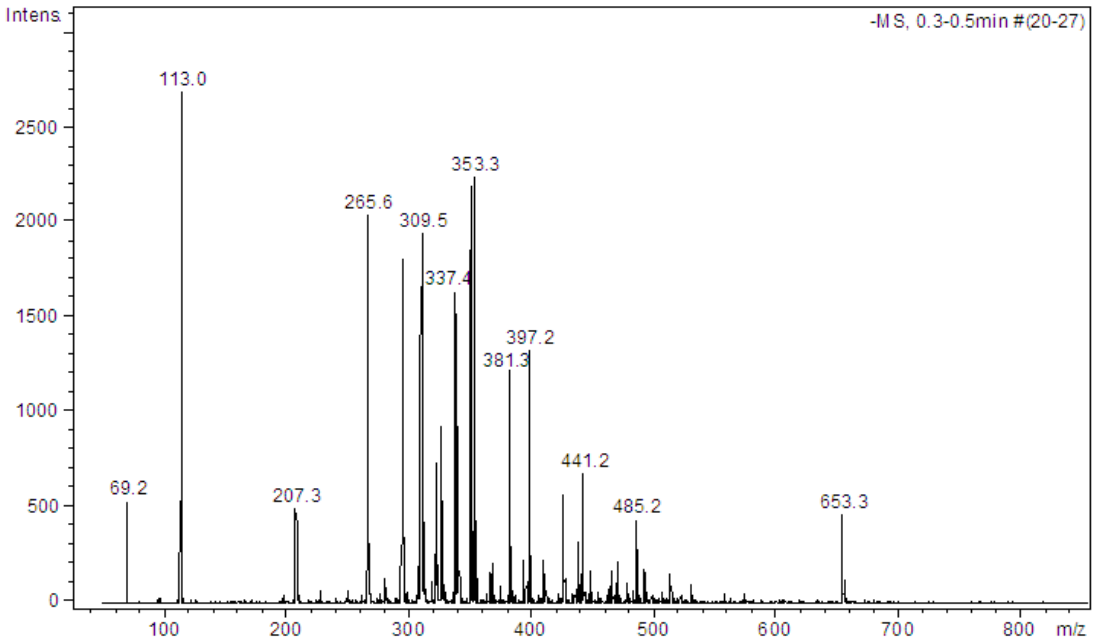

Figure S1B Negative-ion ESI-MS of MimAM(H)-PW

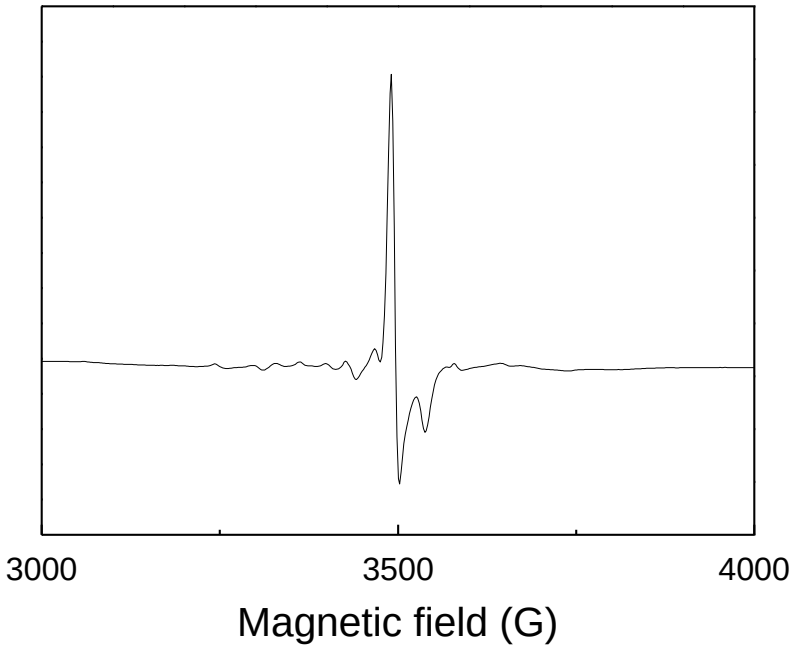

Figure S2 ESR spectrum of MimAM(H)-PW

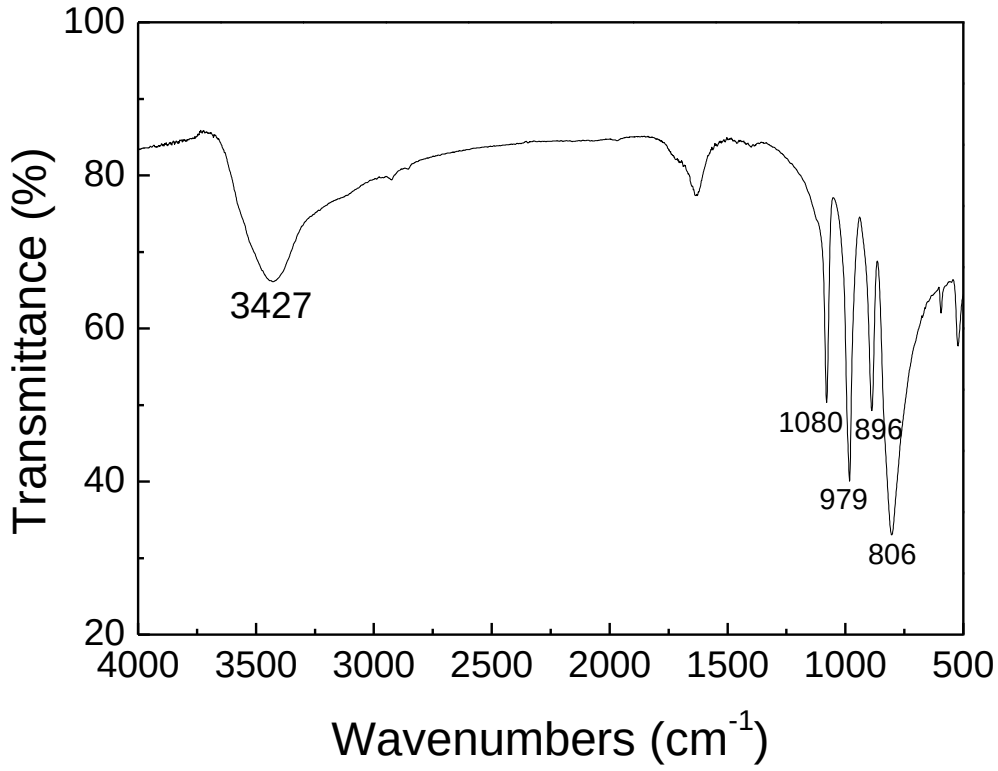

Figure S3A FT-IR spectra of $H_3PW_{12}O_{40}$

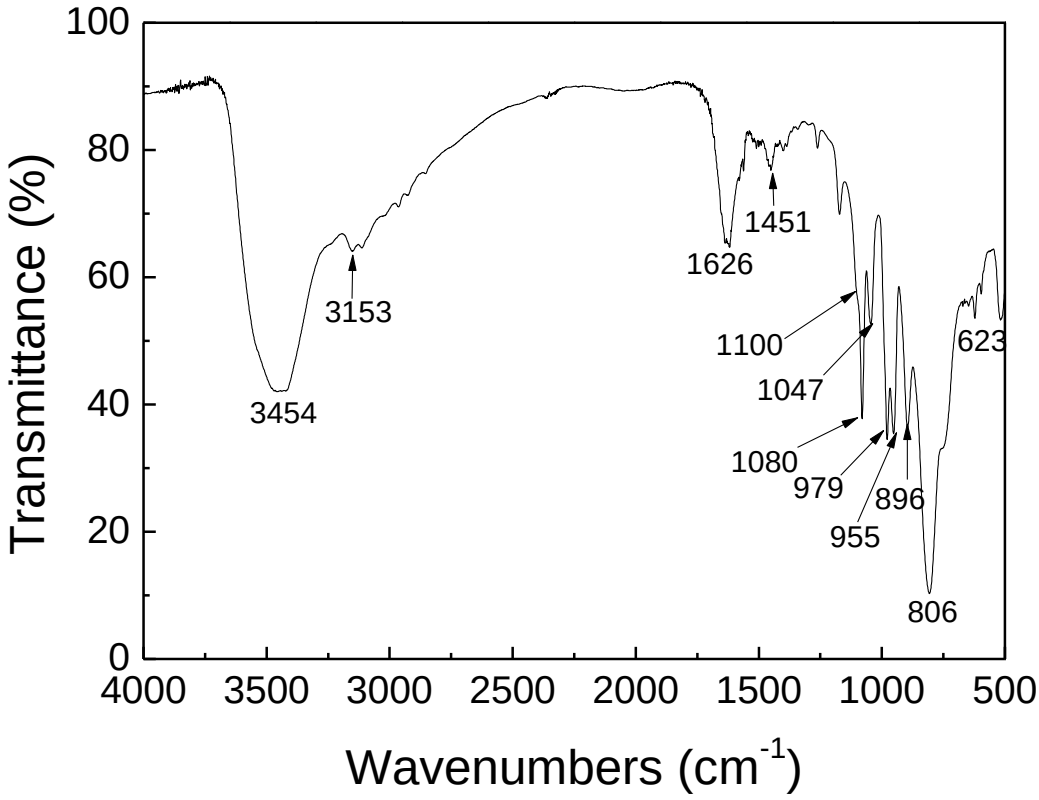

Figure S3B FT-IR spectra of MimAM(H)-PW

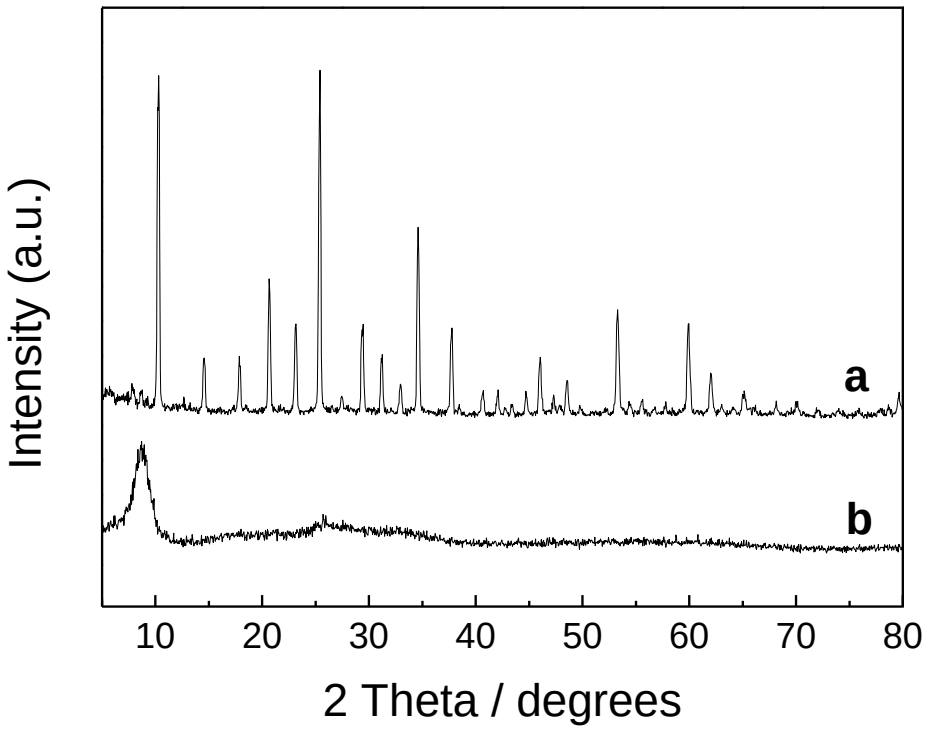

Figure S4 XRD patterns of (a) $H_3PW_{12}O_{40}$ and (b) MimAM(H)-PW

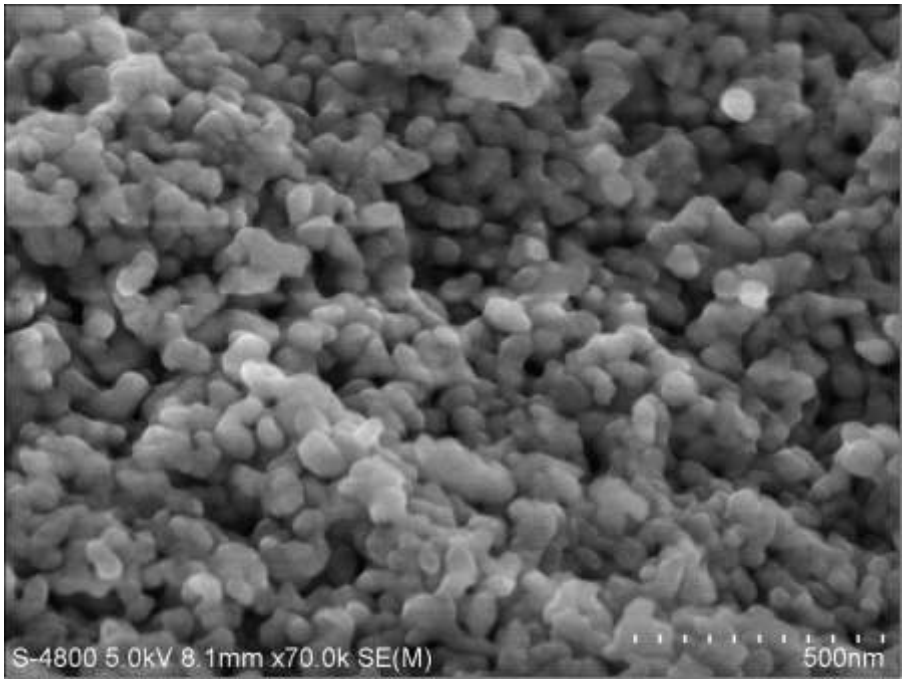

Figure S5 SEM image of MimAM(H)-PW

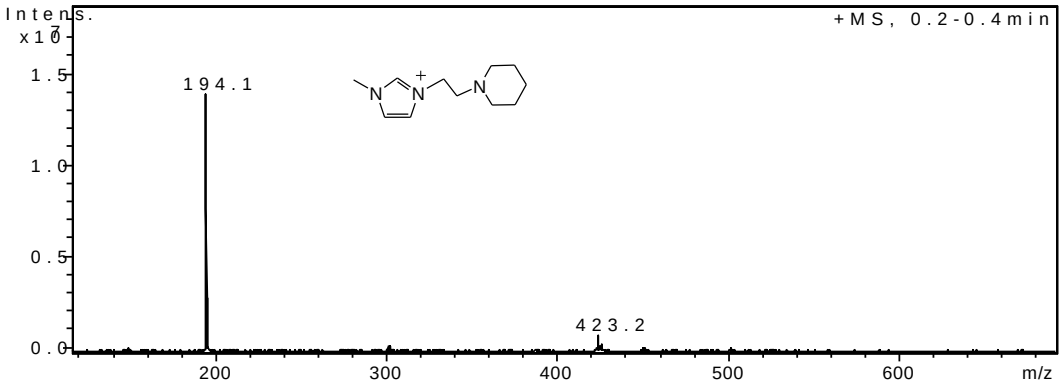

Figure S6A Positive-ion ESI-MS of MimPD(H)-PW

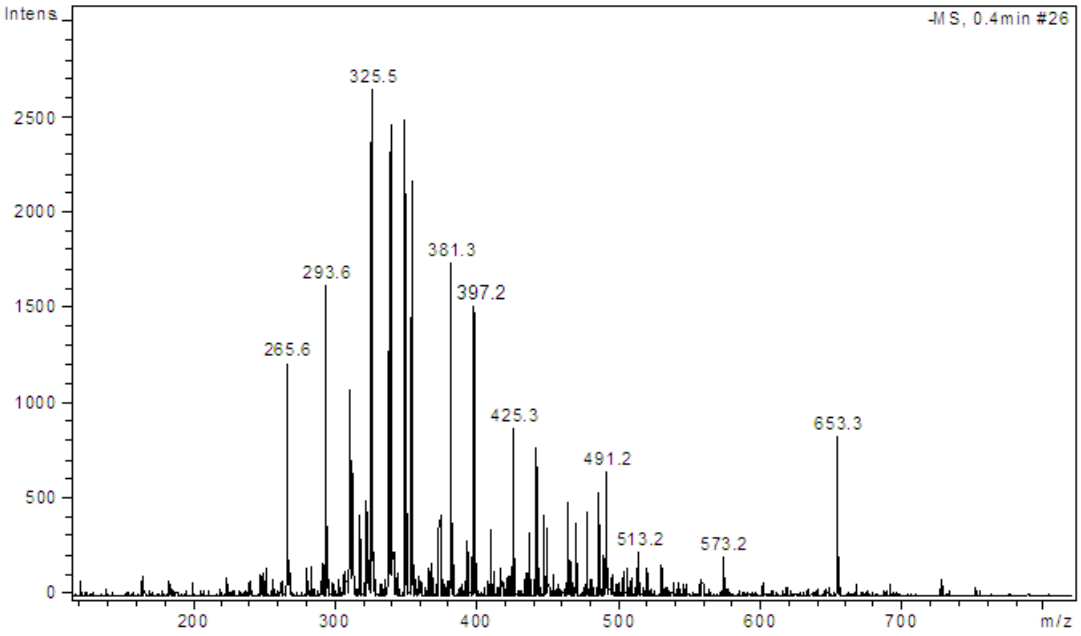

Figure S6B Negative-ion ESI-MS of MimPD(H)-PW

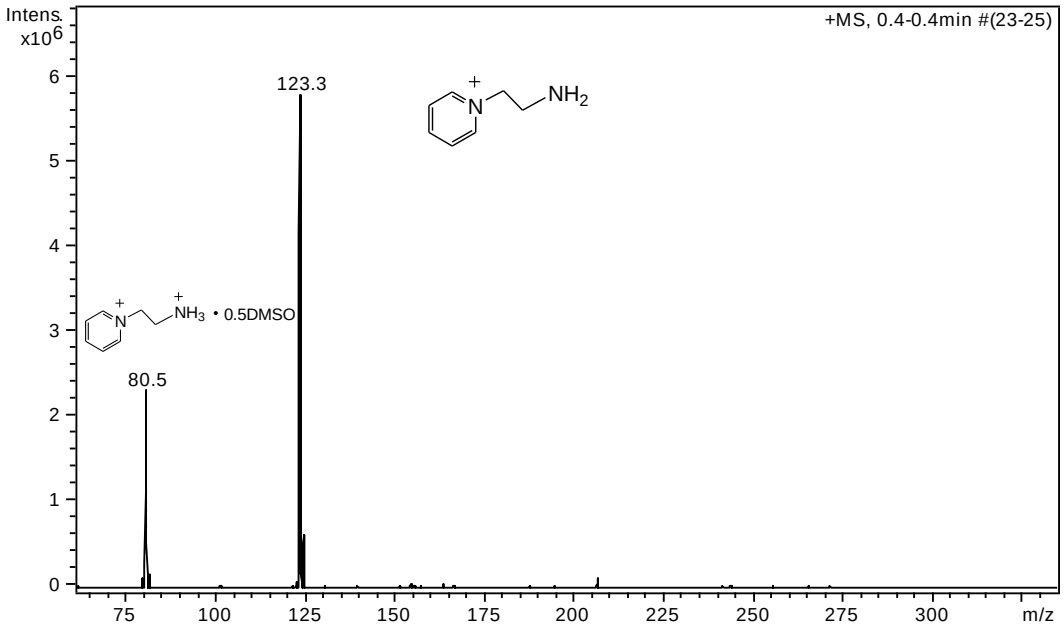

Figure S7A Positive-ion ESI-MS of PyAM(H)-PW

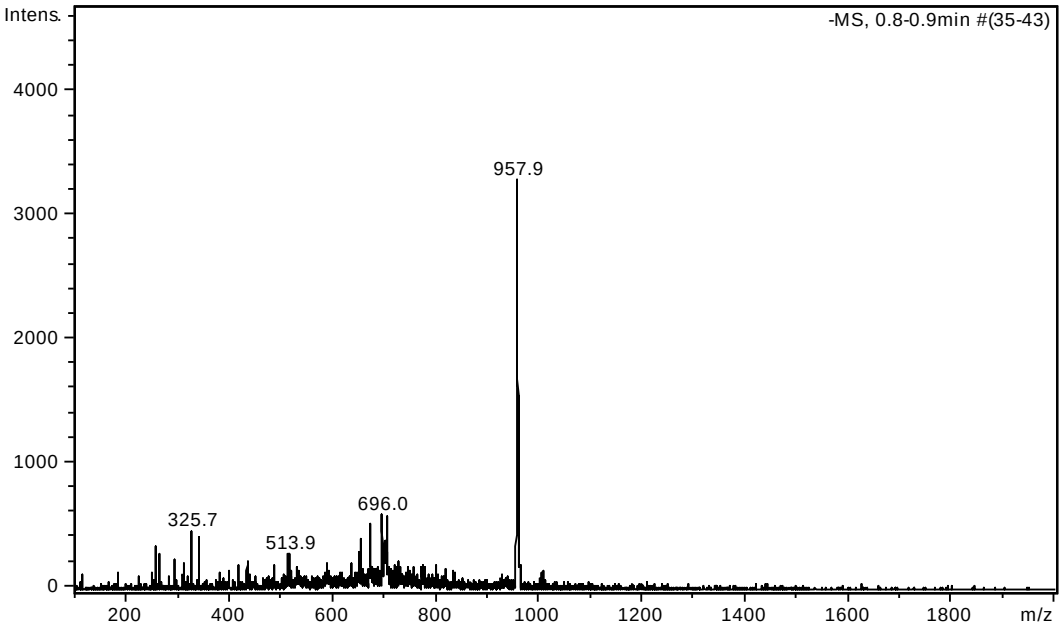

Figure S7B Negative-ion ESI-MS of PyAM(H)-PW

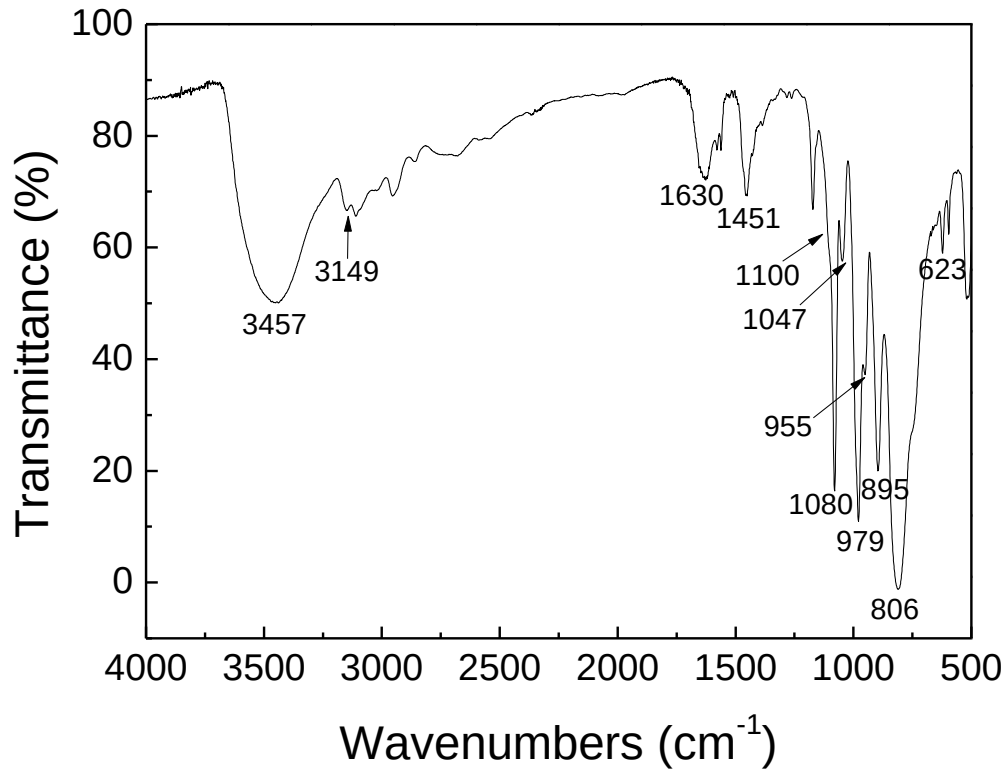

Figure S8 FT-IR spectra of MimPD(H)-PW

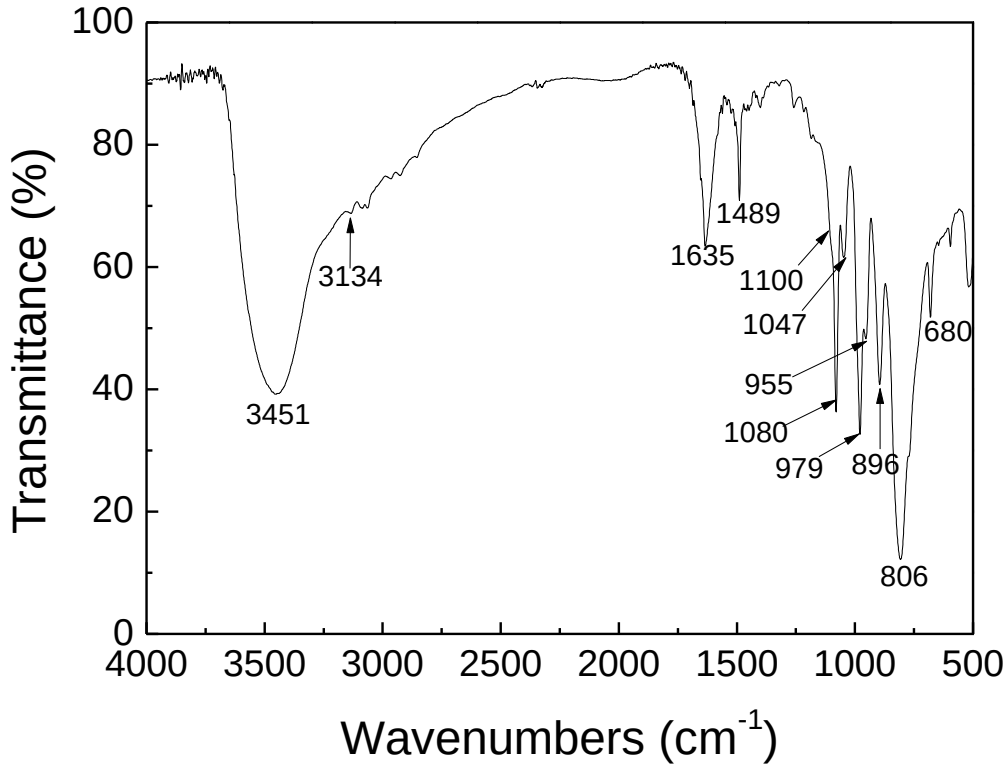

Figure S9 FT-IR spectra of PyAM(H)-PW

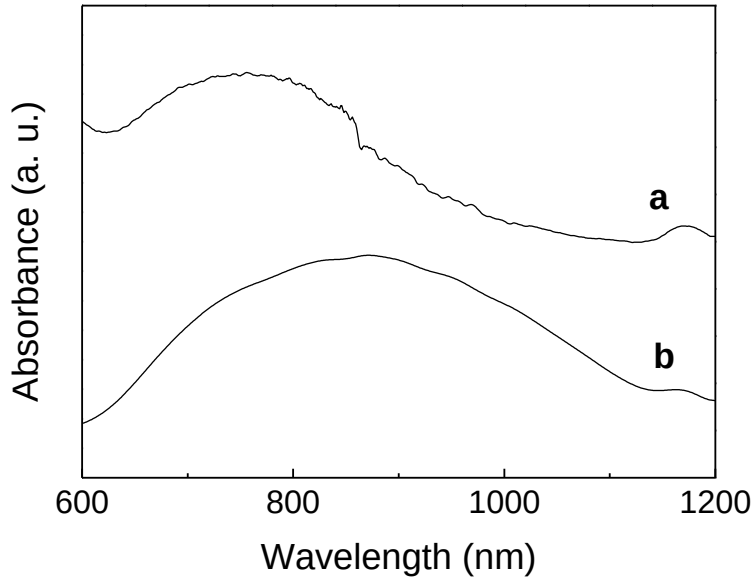

Figure S10 UV-vis spectra of (a) MimPD(H)-PW and (b) PyAM(H)-PW

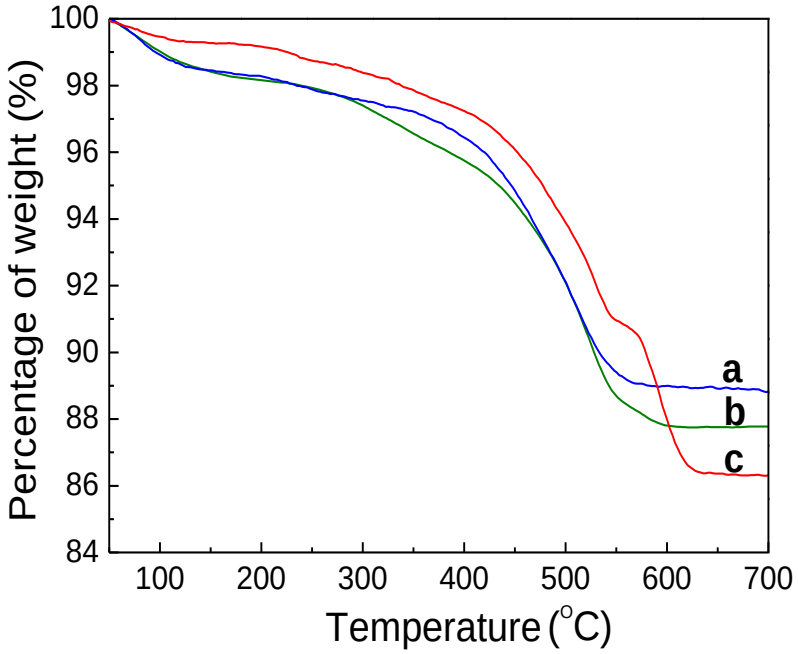

Figure S11 TG curves of (a) MimAM(H)-PW, (b) PyAM(H)-PW, and (c) MimPD(H)-PW